Neuroimaging of the Pituitary Gland
Practical Anatomy and Pathology

Philip R. Chapman, MD*, Aparna Singhal, MD,
Siddhartha Gaddamanugu, MD, Veeranjaneyulu Prattipati, MD

KEYWORDS

• Pituitary adenoma • Macroadenoma • MR imaging • Craniopharyngioma • Meningioma
• Hypophysitis • Apoplexy

KEY POINTS

- MR imaging is the study of choice for evaluating primary tumors and other lesions of the pituitary gland and the central skull base region.
- CT is complimentary in evaluating pituitary and other sellar masses given its ability to detect calcification and assess osseous involvement of skull base.
- The adenoma is the most common lesion of the pituitary gland and can be symptomatic because of its endocrine effects or localized mass effect.
- Macroadenomas can have a variety of imaging appearances based on size, cystic/necrotic change, extent of local invasion, and post-treatment effects.
- There is a broad spectrum of disorders that should be considered in the radiologic evaluation of pituitary, sellar, and suprasellar masses.

INTRODUCTION

The pituitary gland is a small, complex endocrine organ located within the sella of the central skull base. It is anatomically and functionally separated into the anterior lobe (adenohypophysis) and the posterior lobe (neurohypophysis). The anterior lobe produces multiple hormones, including, prolactin, growth hormone (GH), adrenocorticotropic hormone (ACTH), thyroid-stimulating hormone (TSH), follicle-stimulating hormone, and luteinizing hormone. The posterior lobe is an anatomic extension of the hypothalamus and is the site for the secretion of oxytocin and vasopressin. Various pathologic conditions affect the pituitary gland and can produce endocrinologic and neurologic abnormalities. Common lesions include congenital lesions, developmental abnormalities, inflammatory conditions, and a variety of benign and malignant neoplasms. Dedicated MR imaging of the pituitary is the radiologic modality of choice for evaluating the pituitary gland, central skull base, and parasellar regions. Computed tomography (CT) is complementary and allows for identification of calcification and can evaluate osseous integrity of the central skull base. This review emphasizes basic anatomy, current imaging techniques, and highlights the spectrum of pathologic conditions that affect the pituitary gland and sellar region.

ANATOMY

The pituitary gland is a small endocrine gland located in the sella turcica, a saddle-shaped depression in the central sphenoid bone. It is of critical importance to the body's metabolism because it produces, stores, secretes, and regulates several important hormones. The pituitary gland has an anterior lobe (adenohypophysis) and posterior lobe (neurohypophysis). The

Department of Radiology, School of Medicine, University of Alabama Birmingham, 619 19th Street South, JT N419, Birmingham, AL 35249-6830, USA
* Corresponding author. 2912 Tantallon Drive, Hampton Cove, AL 35763.
E-mail address: pchapman@uabmc.edu

Radiol Clin N Am 58 (2020) 1115–1133
https://doi.org/10.1016/j.rcl.2020.07.009

adenohypophysis constitutes 75% of total pituitary volume and is mainly comprised of the pars distalis. Composed of cords of epithelial cells flanked by vascular sinusoids, the adenohypophysis is where most pituitary hormones are synthesized and stored (GH, prolactin, TSH, ACTH, follicle-stimulating hormone, and luteinizing hormone). The pars intermedia is an endocrinologically inactive narrow zone between the adenohypophysis and neurohypophysis and can contain some microscopic remnants of Rathke cleft (**Fig. 1**).

Derived from the neural ectoderm, the neurohypophysis extends from the hypothalamus to the sella. Composed of axons arising from hypothalamic neurons of the supraoptic and paraventricular nuclei, it forms the hypothalamohypophyseal tract. Its distal axonal terminals include neurosecretory granules that contain oxytocin or vasopressin. The presence of vasopressin is presumed to be responsible for the hyperintense signal identified on T1-weighted MR images, the so-called pituitary bright spot, a normal finding of the posterior lobe.

The infundibulum (pituitary stalk) is a linear structure extending from the hypothalamus to the pituitary gland. It is comprised of the anterior pars tuberalis and posterior pars infundibularis. The pars tuberalis is considered to be part of the adenohypophysis. It partially surrounds the pars infundibularis, which contains unmyelinated axons of the hypothalamic neurons that extend to the posterior lobe. The normal stalk has a thickness of approximately 2 mm and should be considered abnormal if it measures greater than or equal to 4 mm.

The size of pituitary gland is variable and depends on age and physiologic status. The pituitary size is roughly estimated by its height, and its height is routinely measured from coronal or sagittal MR images. Pituitary dimensions in selected age and gender groups are depicted in **Table 1**. Note the gradual decrease in size of the pituitary gland in elderly patients.[1]

A thin horizontally oriented dural sheet that stretches across the top of the sella, the diaphragma sellae, separates the sella from suprasellar space. The diaphragma sellae is mildly convex inferiorly and contains a variable-sized central opening or perforation that allows the passage of the pituitary stalk. The diaphragma sellae is attached to the clinoid processes and contiguous with the dural covering of the cavernous sinus roofs bilaterally.

Blood supply to the anterior pituitary is unique and complex. The adenohypophysis lacks a direct blood supply and most of the blood reaches the parenchyma through the hypothalamic hypophyseal portal system. Small branches from superior hypophyseal artery enter the median eminence of the hypothalamus and form a primary capillary plexus. The primary plexus is connected to portal veins that extend through the infundibulum to the adenohypophysis. This portal venous system supplies most of the blood to the adenophyphysis and allows for precise hormonal regulation between the hypothalamus and the pars distalis (**Fig. 2**). The posterior pituitary has direct blood supply

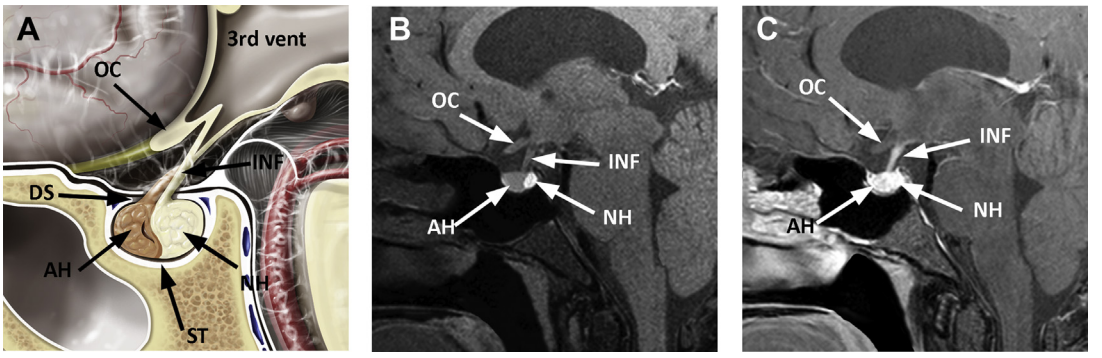

Fig. 1. Normal sagittal anatomy. (*A*) Sagittal graphic demonstrates key structures including the sella turcica (ST), the anterior pituitary or adenohypophysis (AH), posterior pituitary or neurohypophysis (NH), the pituitary stalk or infundibulum (INF), diaphragma sella (DS), and optic chiasm (OC). (*B*) Sagittal fat-saturated T1-weighted MR imaging without gadolinium shows hyperintense signal in neurohypophysis, a normal finding referred to as the pituitary bright spot. Note the relationship of the sella turcica to the sphenoid sinus and clivus. (*C*) Sagittal postgadolinium T1-weighted image shows homogeneous enhancement of the infundibulum and anterior pituitary. ([*A*] *From* Osborn AG, Salzman KL, Jhaveri MD, Barkovich AJ. Diagnostic Imaging : Brain. 2015; with permission.)

Table 1
Pituitary gland: age/physiologic status, sex, and size

Age Group/Physiologic Status	Sex	Size (mm)
Prepubertal children	Either	2–6
Prepubertal children	Boys	7–8
	Girls	8–10 (round shape)
Third trimester pregnancy	Women	10
First week postpartum	Women	12
Adult, aged ≥50 y	Men	8
	Women	8

from the inferior hypophyseal artery, which arises from internal carotid artery (ICA). The intrinsic pituitary capillaries are unique in that they are fenestrated and are outside of the blood-brain barrier. Therefore, the pituitary gland homogeneously enhances after administration of intravenous contrast agents.

TECHNIQUE

Dedicated MR imaging of the pituitary gland and sella is the modality of choice for evaluating intrinsic lesions of the pituitary gland, such as adenomas and other lesions localized to the sella. Excellent spatial resolution and multiplanar technique allows for complete evaluation of the lesion and is necessary for treatment or surgical planning. Sagittal and coronal planes are preferred, typically using 2- to 3-mm slice thickness. Routine imaging with a 1.5-T magnet is generally satisfactory. However, the 3-T MR imaging magnet can offer an advantage of increased sensitivity for microadenomas and is recommended if there is strong clinical suspicion of an adenoma and an initial negative scan using 1.5 T.[2,3]

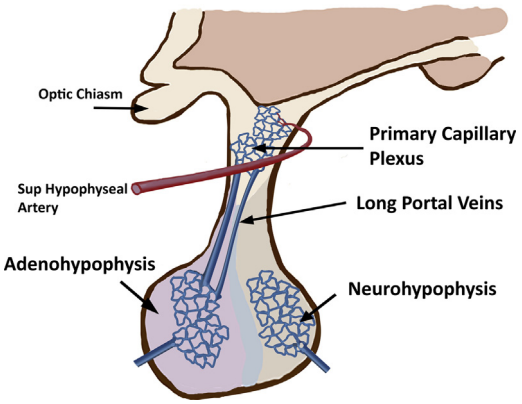

Fig. 2. Schematic diagram depicts the blood supply to the adenohypophysis. Blood enters the hypothalamus at the median eminence by way of branches from superior hypophyseal artery. Within the inferior hypothalamus, there is a primary capillary venous plexus. This is connected to the venous plexus of the pars distalis by way of interconnecting long portal veins that extend through the hypothalamus. The neurohypophysis receives blood primarily through the inferior hypophyseal vessels, and hormones are secreted in this region via terminal axons that originate from the hypothalamus.

A dedicated pituitary protocol includes precontrast sagittal and coronal T1-weighted images, followed by postgadolinium sequences in same plane. A T2-weighted coronal sequence with fat saturation also is beneficial. The normal adenohyphysis is isointense to brain on routine T1-weighted and T2-weighted images. The posterior pituitary generally contains the pituitary bright spot, if normal. The infundibulum and gland enhance homogeneously after contrast administration. Using such techniques, most adenomas and other sellar pathologies are diagnosed with a high degree of sensitivity. Depending on the circumstances and institutional preferences, optimal evaluation of the whole brain includes performance of axial fluid-attenuated inversion recovery, diffusion-weighted, and whole-brain postgadolinium sequences.

Dynamic MR imaging is a useful technique that is particularly beneficial for identifying microadenomas. Dynamic sequences take advantage of the fact that adenoma tissue enhances more slowly than normal pituitary tissue. If sequential images are obtained in rapid succession during the first-pass arterial phase, a microadenoma is identified as a small focus of nonenhancing tissue against a background of normally enhancing pituitary gland (**Fig. 3**).

Optimization of dynamic sequence with 3-mm thin coronal slices, small field of view (12 × 12 cm), fine matrix size of 256 × 192, and use of spoiled gradient echo techniques instead of spin echo T1 is helpful.[4,5] Dynamic sequences should be acquired every 30 seconds for 3 minutes

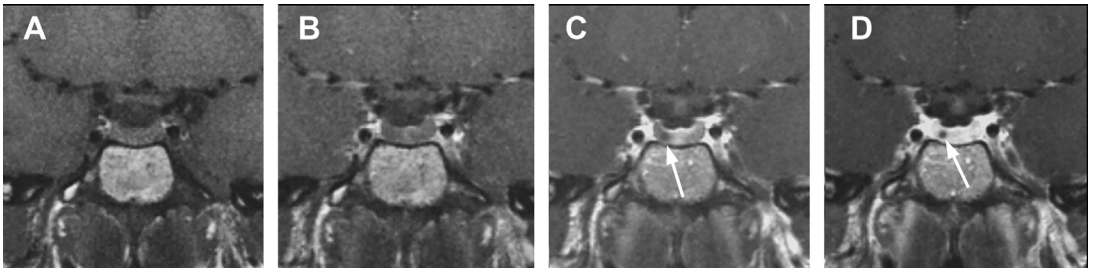

Fig. 3. Sequential same-slice T1-weighted coronal images through anterior pituitary gland during contrast injection of gadolinium. Precontrast and earliest arterial phase contrast images show no obvious abnormality (*A*, *B*). During contrast infusion, a small hypodense region in right side of the gland (*arrows*, *C*, *D*) shows hypoenhancement relative to normal pituitary, consistent with microadenoma.

with five slices/acquisition.[6] The pituitary shows rapid and progressive enhancement usually beginning superiorly and extending inferiorly through the entire gland. Delayed postcontrast images are then obtained in sagittal and coronal planes. On delayed sequences, small adenomas may be isointense to pituitary gland and difficult to see. As new sequences have been developed, some studies have questioned the routine role of dynamic imaging, arguing that other sequences, such as enhanced three-dimensional spoiled gradient echo, may be as sensitive or better.[7]

Diffusion-weighted imaging is not routinely performed for pituitary lesions, but studies are under way to evaluate its utility for sellar and suprasellar lesions. It is challenging because of inhomogeneity at the skull base from air-bone interface from routine echoplanar diffusion imaging. Non–echoplanar diffusion imaging diffusion techniques, such as propeller diffusion-weighted imaging (General Electric, Boston, MA) or BLADE (Siemens, Munich, Germany), are used. Diffusion may help differentiate Rathke cleft cysts from other suprasellar/intrasellar lesions.[8] Some authors suggest that pituitary apoplexy may be detected early using diffusion-weighted MR imaging.[9] Pituitary adenomas with lower apparent diffusion coefficient values correlate with higher collagen content and may have surgical implications.[10] However, perfusion and spectroscopy have limited roles in sellar imaging and are not routinely performed.[11]

High-resolution CT scanning is complementary and may be used primarily if MR imaging is contraindicated. CT allows for identification of any intrinsic calcification/ossification of the lesion, can help in narrowing the differential, and is excellent for evaluating the osseous integrity of the central skull base. CT can be performed with 1-mm axial thin slices with contrast for best spatial resolution. Coronal and sagittal reformats should be obtained.[1,2,4,5,10–14] CT angiography is also complementary, especially in cases where a parasellar vascular lesion, such as aneurysm, is considered.

ADENOMA

The benign adenoma represents the most common pituitary neoplasm and arises from the adenohypophysis. These are benign epithelial lesions and account for about 10% to 15% of all intracranial tumors. Pituitary adenomas occur across a wide age spectrum, from childhood to the elderly. It has been estimated from postmortem and other clinical studies that pituitary adenomas occur in approximately 20% of the normal population, but many are incidental and asymptomatic. Adenomas are most often classified according to hormonal production and size, which predominantly determines the clinical presentation. They can also be classified based on histology and biologic behavior.[14]

Adenomas that are hormone-producing are said to be endocrinologically active or functional, whereas nonfunctional tumors produce no measurable hormone. Prolactinomas are the most common hormone-secreting tumors and account for about 30% of all pituitary adenomas. Nonfunctioning adenomas are the second most common tumors, comprising 25% to 30% of pituitary adenomas.[15]

Microadenoma

Adenomas are unencapsulated tumors, and as they begin to grow they initially infiltrate the parenchyma of pituitary gland itself. Lesions measuring less than 1 cm in size are called microadenomas. These lesions are generally confined to the pituitary gland/sella. In this case, symptoms are not related to the size of the lesions but rather the possible excess production of hormone.

On T1- and T2-weighted images, microadenomas may be isointense to normal pituitary gland. Microadenomas enhance variably with contrast but generally enhance at a slower rate than normal pituitary tissue. Dynamic enhanced images are performed to take advantage of this early differential enhancement and are generally considered to be the most sensitive sequence for microadenoma detection. Using high-resolution techniques, MR imaging can detect adenomas as small as 2 mm. Some institutions perform dynamic imaging routinely as part of pituitary protocol when adenoma is suspected. Others reserve dynamic sequences for cases where adenomas are suspected but conventional imaging is negative, especially in cases of suspected ACTH-secreting tumors, which are typically small, averaging 5 mm in diameter.[6]

Macroadenoma

Macroadenomas are adenomas measuring greater than or equal to 1.0 cm. On unenhanced CT, macroadenomas generally demonstrate a soft tissue mass in the sella that is isodense with gray matter and not clearly discrete from the gland itself. Lesions may show variable attenuation because of cyst formation or necrosis. Occasionally, hemorrhage results in hyperdensity of the lesion. Generally, adenomas do not calcify; however, calcification is seen in 1% to 2%. Postcontrast CT shows moderate, inhomogeneous enhancement.

MR imaging appearance varies according to sequence. T1-weighted images show a lesion isointense to gray matter. T1 hyperintensity seen occasionally in the setting of subacute hemorrhage and intratumoral hemorrhage occurs in up to 10% to 15% of adenomas. The pituitary bright spot is displaced superiorly above the diaphragma sellae in 80% of cases, but may also be absent with larger adenomas. Following contrast, most adenomas demonstrate heterogeneous enhancement. Ultimately, tumors may grow beyond the pituitary capsule and can extend beyond the confines of the sella. In general, macroadenomas can extend superiorly into the suprasellar cistern; laterally into the cavernous sinus; or inferiorly into the sellar floor, clivus, or sphenoid sinus.[16]

Suprasellar Extension

Classically, macroadenomas follow a path of least resistance: tumor growth occurs through the central opening in the diaphragma sellae into the suprasellar cistern. The circumlateral leaflets of the diaphragma sellae are initially displaced upward and can create a horizontal restriction of tumor growth, leading to the typical bilobed appearance in the coronal plane, with the lower sellar component of tumor separated partially from its upper suprasellar component. The classic appearance has been likened to a snowman (**Fig. 4**). As tumor extends superiorly, microscopic invasion of the diaphragma sellae itself often occurs.[17]

As tumor enlarges and extends vertically, it can contact, efface, displace, or compress the optic chiasm. Compression of the optic chiasm can produce a variety of visual deficits, including chiasmal syndrome.[18] Pituitary adenomas are the most common lesions that produce chiasmal syndrome, followed by other lesions that cause extrinsic optic chiasm compression, such as meningiomas or craniopharyngiomas. Although bitemporal hemianopsia, defect of impaired peripheral vision in the temporal (outer) halves of the visual field of each eye, is often suggested as a classic finding associated with pituitary adenoma, actually it is rare. Rather, patients more often present with incomplete bitemporal visual defects or mixed defects.[19]

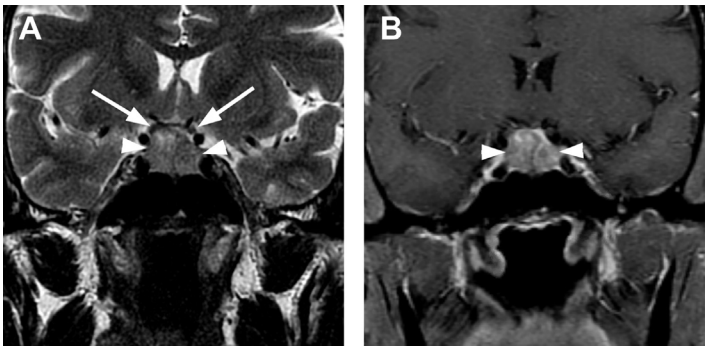

Fig. 4. Nonsecreting pituitary adenoma. This lesion was discovered incidentally in 55-year-old man with no endocrine abnormalities or visual symptoms. (*A*) Coronal T2-weighted image shows a sellar mass (*arrowheads*) extending into the suprasellar region. The lesion minimally splays the proximal cisternal optic nerves (*arrows*). (*B*) Coronal postgadolinium T1-weighted image demonstrates heterogeneous enhancement of the macroadenoma (*arrowheads*). A subtle waist is formed at the level of the diaphragma sellae.

There is no consensus on how best to measure the extent of suprasellar extension or the degree of optic chiasm displacement or compression. However, in general, the larger the tumor and greater the chiasm compression, the more likely the patient is to have more significant visual deficits.

Although no consensus exists, several radiologic reports in the past have used the term "giant macroadenoma" for a mass that exceeds 40 mm in greatest dimension. Symon and colleagues[20] defined giant adenomas as those with an extension of more than 40 mm from the midline of planum sphenoidale in any direction or suprasellar extension to within 6 mm of the foramen of Monro. Other authors have reserved this term for tumors where the superior margin exceeded 20 mm above the planum sphenoidale. Giant macroadenomas are generally regarded as more aggressive, more difficult to resect, and more likely to recur (**Fig. 5**).[21]

Cavernous Sinus Invasion

Approximately 5% to 10% of all pituitary adenomas extend laterally beyond the margins of the adenohypophysis and sella, invading the adjacent cavernous sinus. Involvement of the cavernous sinus increases surgical procedure complexity, results in higher rates of residual/recurrent tumor, and is associated with persistent endocrine dysfunction. Definitions of cavernous sinus invasion have been variably based on radiologic, surgical, endoscopic, and microscopic criteria.

The microscopic interface between the pituitary and the cavernous sinus has been evaluated through histologic and microdissection techniques. Songtao and colleagues[22] considered the outer pituitary wall as a two-layered membrane: an inner lamina propria adherent to the pituitary tissue; and a looser, outer pituitary capsule. The outer layer also serves as part of the medial wall of the cavernous sinus. In their description, the medial wall of the cavernous sinus consisted of a fibrous layer in addition to the pituitary capsule. As tumor extends laterally from the sella, it crosses the lamina propria, the pituitary capsule, the fibrous layer of the cavernous sinus, and finally, the endothelial lining of the venous compartment. The authors found that superior margin is thinner, which might explain why adenomas more often extend into the superior compartment of the cavernous sinus.[22]

MR imaging is not reliable at distinguishing these microscopic layers separating the laterally convex pituitary gland from the medial cavernous sinus. MR imaging evaluation of invasion relies on macroscopic findings, such as the relationship of tumor to the cavernous ICA and extent of

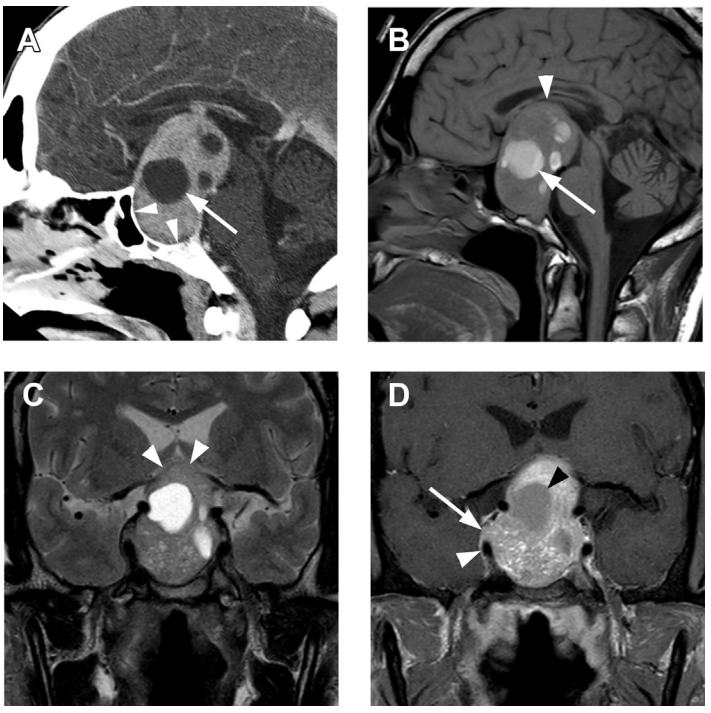

Fig. 5. Giant macroadenoma. A 43-year-old man presents with 2-week history of severe visual loss of left eye. (*A*) Sagittal reformatted contrast-enhanced CT scan shows a 6.0-cm mass with several cysts (*arrowhead*) expanding but not destroying the sella (*arrowheads*) and compressing the anterior third ventricle. (*B*) Sagittal unenhanced T1-weighted image shows giant macroadenoma with cystic areas (*arrow*) that contain proteinaceous contents and demonstrate T1 shortening. The lesion compresses the anterior third ventricle superiorly (*arrowhead*). (*C*) Coronal T2-weighted image shows a classic snowman appearance of the mass. The optic chiasm is severely compressed and not identified as distinct structure (*arrowheads*). (*D*) On coronal contrast-enhanced T1-weighted image, the solid portions of the lesion show moderate enhancement, whereas the cystic areas (*black arrowhead*) maintain some T1 hyperintensity. The lesion expands the sella and extends into the right cavernous sinus (*arrow*) passing above the cavernous ICA (*white arrowhead*).

cavernous sinus involvement. In 1993, Knosp and colleagues[23] introduced an MR imaging–based classification system to predict cavernous sinus invasion. This system was based on lateral tumor extent in relationship to a series of tangential lines drawn between the intracavernous and supracavernous ICAs seen on coronal MR images. This classification system defined five grades of invasion, ranging from 0 to 4 (**Fig. 6**). The data showed that identification of tumor past the intercarotid line (grade 2 and higher) on coronal MR imaging was highly predictive of cavernous sinus invasion identified at surgery. Conversely, patients with grade 0 or grade 1 were unlikely to have definitive invasion. Their results also showed that the degree of cavernous invasion was directly related to tumor size.

The Knosp-Steiner classification of potential cavernous sinus invasion by macroadenoma (see **Fig. 6**) involves using coronal MR imaging to determine extent of lateral tumor growth in relationship to tangential lines drawn between the cavernous ICA and supraclinoid ICA.

Others have evaluated the Knosp-Steiner macroadenoma classification and other MR imaging findings that might predict the presence of cavernous sinus invasion. Cottier and colleagues[24] found the most specific sign of cavernous sinus invasion to be partial tumor encasement of the intracavernous ICA, defined as involvement of 67% of its circumference (positive predictive value of 100%). Macroadenomas with Knosp-Steiner grade of 3 had a positive predictive value of 85%. Invasion is highly probable (positive predictive value of 95%) if the carotid sulcus venous compartment (medial venous compartment inferior to the cavernous ICA on coronal MR imaging) is obliterated. Cavernous sinus invasion could be ruled out with a negative predictive value of 100% if the percentage of encasement of the perimeter of intracavernous ICA was lower than 25% or with Knosp-Steiner grade of 0 or 1 (**Fig. 7**).

Skull Base Invasion

Adenomas that originate in or involve the inferior aspect of the gland and sella can involve the underlying dura and bone of the central skull base. Selman and colleagues[25] performed transphenoidal surgery for pituitary adenoma in 65 patients and reported that 51 (85%) demonstrated microscopic dural invasion of the sellar floor. These authors demonstrated a direct correlation between overall tumor size and the presence of dural invasion. Dural invasion was present in 95% of cases of macroadenoma (>10 mm). The authors also noted that microscopic dural invasion occurred even in some microadenomas. Meij and colleagues,[26] in a larger study of 354 patients, found dural invasion in 45% of all cases and confirmed a correlation between tumor size and dural invasion.

As the macroadenoma infiltrates the gland, generalized expansion of the sella can occur, often with preservation of smooth cortical margins of the bony sella. With progressive enlargement, cortical thinning of the underlying bone can occur and is most often identified along the roof of the sphenoid sinus. Focal dehiscence of the sphenoid roof can occur, and the tumor can protrude directly into the sphenoid sinus (**Fig. 8**). The tumor can also infiltrate into the

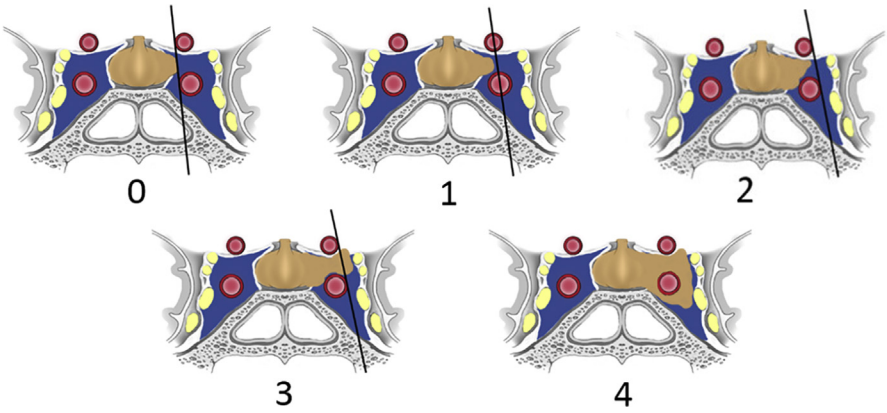

Fig. 6. The Knosp-Steiner classification of potential cavernous sinus invasion by macroadenoma. This involves using coronal MR imaging to determine extent of lateral tumor growth in relationship to tangential lines drawn between the cavernous ICA and supraclinoid ICA. The classification ranges from 0 to 4 and expresses likelihood of cavernous sinus invasion that would be encountered at surgery. Stage 0 is unlikely to correlate with tumor invasion. Stage 4 demonstrates encasement of the cavernous ICA, a definitive finding for tumor invasion.

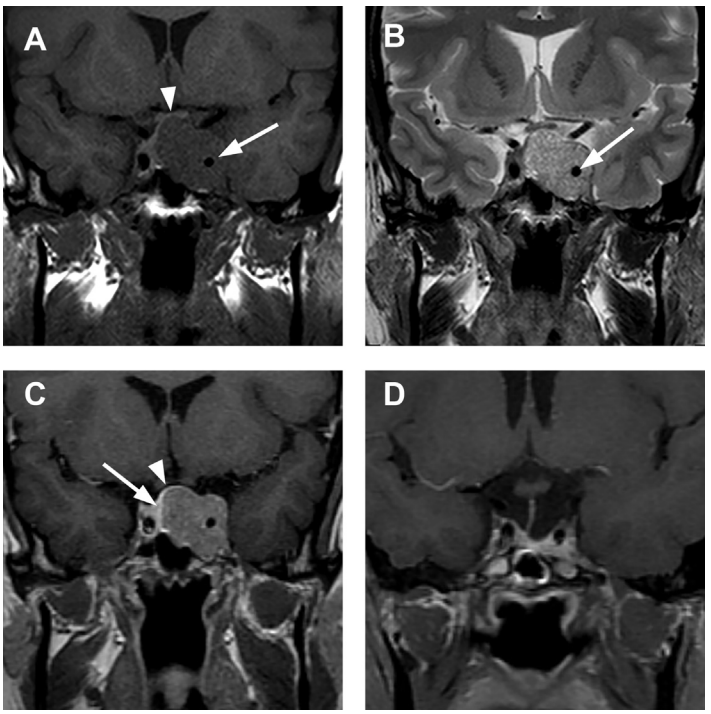

Fig. 7. ACTH-secreting macroadenoma. A 33-year-old woman presented with clinical findings and biochemical evidence of Cushing disease. (*A*) Unenhanced coronal T1-weighted MR imaging shows large left-sided sellar mass with suprasellar extension and left cavernous sinus invasion. There is mild compression of the optic chiasm (*arrowhead*) and encasement of the cavernous ICA (*arrow*). (*B*) Coronal T2-weighted image shows heterogeneously hyperintense mass with left cavernous ICA encasement (*arrow*). (*C*) Coronal postcontrast T1-weighted MR image shows solid heterogeneously enhancing sellar mass that measures $3.0 \times 2.7 \times 2.5$ cm. The mass displaces the normal pituitary (*arrow*) and infundibulum (*arrowhead*) to the right. (*D*) Postoperative coronal image shows satisfactory resection of the large lesion despite the cavernous sinus invasion.

trabecular bone and marrow space of the clivus. In rare instances, the inferior growth pattern can dominate (Fig. 9). The bony change of the clivus can include focal irregularity, permeative change, mixed sclerotic-permeative change, or frank lysis. Large tumors can expand and destroy the clivus, mimicking chordoma, myeloma, or metastatic disease. Most reports of infrasellar invasion are small case series or case reports. Luo and colleagues[27] reported 28% incidence of infrasellar extension with involvement of the floor of the sella and sphenoid sinus.

Chen and colleagues[28] recently evaluated clival invasion of pituitary macroadenomas using CT in 390 patients. Thirty-two patients (8.21%) had clival invasion detected by CT and confirmed at surgery. In this study, the authors found female sex to be the strongest risk factor for clival invasion. This finding contradicted previous studies that suggested a greater propensity of clival invasion in men. As with cavernous sinus invasion, larger tumor volume was found to be a strong risk factor for clival invasion. In this report, clival invasion was more frequent in null-cell adenomas even after correction for larger average tumor volume. Some macroadenomas have a preferential invasion for the central skull base. The tumor is mistaken for a primary sphenoid bone lesion encroaching on the floor of the sella. In these cases, identification of tumor contiguity with the

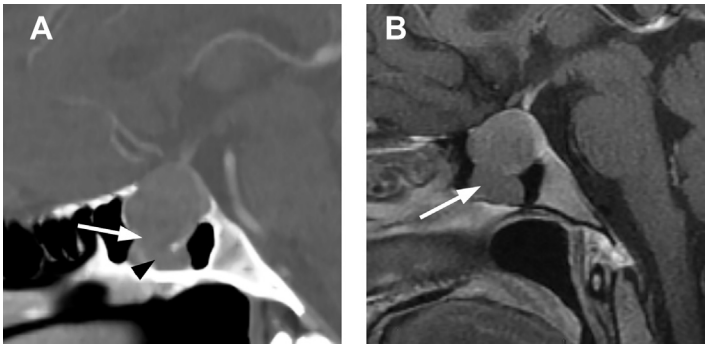

Fig. 8. Macroadenoma invasive to sphenoid sinus. (*A*) Sagittal postcontrast CT reformation with bone windows shows an expansile mass of the sella with dehiscence of the sellar floor (*arrow*) and soft tissue mass in the ventral sphenoid sinus (*arrowhead*). (*B*) Sagittal postcontrast T1-weighted MR imaging shows that there is significant inferior vector of tumor growth (*arrow*). The pituitary gland is not identified as a separate structure from the main mass.

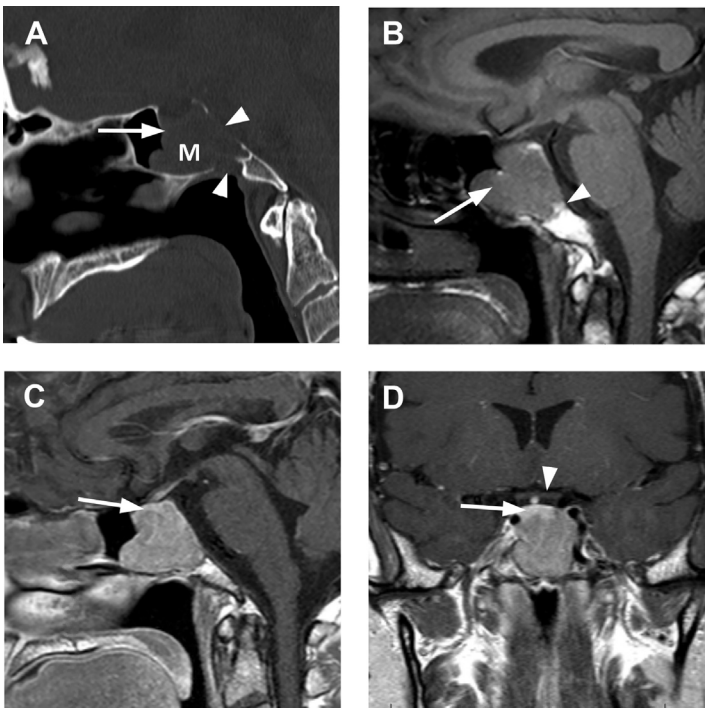

Fig. 9. Nonsecreting macroadenoma invasive to the clivus. (*A*) Sagittal reformation CT scan with bone windows reveals a large invasive soft tissue mass (M) that involves the sella, sphenoid sinus, and clivus. There is dehiscence of the sellar floor (*arrow*) and cortical erosions of the clivus (*arrowheads*). (*B*) Sagittal unenhanced T1-weighted image shows the ventral extension to the sphenoid sinus (*arrow*), and there is demarcation of the inferior margin (*arrowhead*) from normal residual fatty marrow of the clivus. (*C*) Sagittal postcontrast T1-weighted image shows homogeneous enhancement of the tumor that blends with residual normal pituitary superiorly (*arrow*). (*D*) Although there is some suprasellar extension, the major vector is inferiorly, and the chiasm (*arrowhead*) is not compressed. Some residual normal pituitary tissue is seen along upper edge of pituitary (*arrow*).

inferior pituitary gland is the best clue to its pituitary origin.

Pituitary Tumor Apoplexy

Pituitary tumor apoplexy is a clinical syndrome that occurs when an existing pituitary adenoma undergoes an acute hemorrhage or infarction, or both.[29] Most cases occur in males during the fifth or sixth decade of life, and most often occur in previously undiagnosed nonfunctioning pituitary adenomas or prolactinomas.[30] Patients typically present with an abrupt onset of severe headache, variable visual disturbance (including vision loss, field defects, and ophthalmoplegia), and acute hypopituitarism. Radiologic studies are performed as an adjunct to clinical findings to exclude other etiologies and to confirm the presence of a hemorrhagic pituitary lesion. Unenhanced CT is often the first study performed in an acute setting and may demonstrate a variably hyperdense mass of the sella and suprasellar region. With sensitivity greater than 90%, MR imaging is the preferred study of choice and can identify the adenoma, the intrinsic hemorrhage, and necrosis, and evaluate effects on adjacent structures.[31,32]

MR imaging generally demonstrates a sellar mass with variable and complex signals on T1- and T2-weighted images. Imaging findings depend on several factors, including size of the underlying tumor, extent of hemorrhage or necrosis, and timing of the examination. Like hemorrhage elsewhere in the brain, MR imaging appearance varies depending on the sequence and stage of the hemorrhage (hemoglobin degradation). Typically, a sellar and suprasellar mass shows significant regions of T1 hyperintensity, T2 hypointensity, and nonenhancing necrotic tissue centrally (**Fig. 10**). Some peripheral nodular enhancing tissue is identified to confirm presence of underlying adenoma.[33]

PITUITARY CARCINOMA

Pituitary adenomas are benign tumors but can demonstrate aggressive or invasive features. Tumors are considered aggressive if the growth rate is greater than usual or if the tumor progresses despite satisfactory treatment.[34] Pituitary carcinomas are rare, accounting for 0.1% of pituitary tumors.[27] Unlike many other situations, the term carcinoma in this case is applied when adenomas demonstrate aggressive biologic behavior and evidence of metastatic disease. The distinction is not based on histologic criteria. Rather, a tumor of pituitary origin is classified as a carcinoma when there is evidence of noncontiguous leptomeningeal spread to the intracranial compartment or

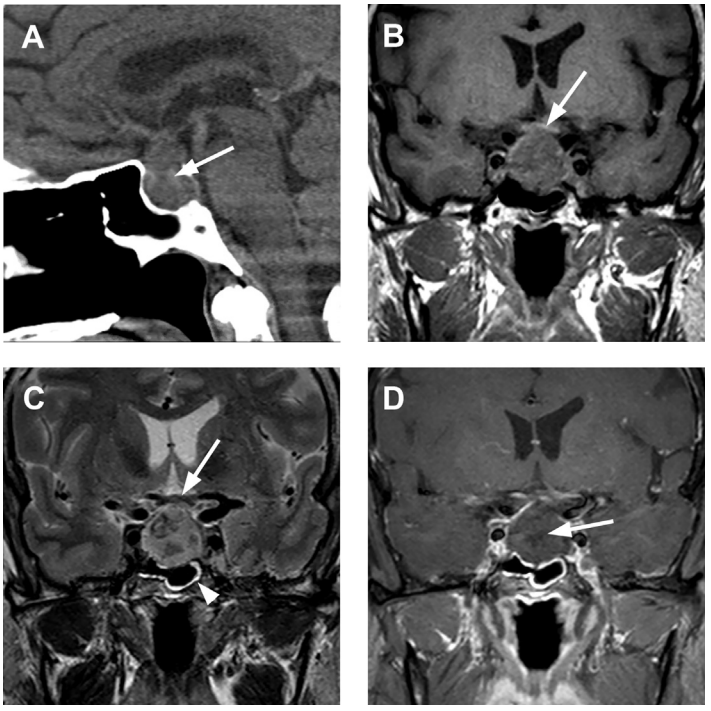

Fig. 10. Pituitary tumor apoplexy in nonfunctioning adenoma. A 65-year-old woman presents with acute onset of headache, nausea, and vomiting, and pituitary insufficiency was detected by laboratory evaluation. (*A*) Sagittal unenhanced CT scan demonstrates an expansile sellar and suprasellar mass (*arrow*). (*B*) Coronal T1-weighted MR image shows that the mass contacts the optic chiasm (*arrow*). (*C*) Coronal T2-weighted image shows that the mass contacts the optic chiasm (*arrow*). There is mild mucosal edema in sphenoid sinus (*arrowhead*). There are areas of intrinsic T2 hypointensity within the mass, consistent with hemorrhage. (*D*) Coronal postcontrast image shows large zone of centrally necrotic tissue (*arrow*), consistent with hemorrhage and/or infarction.

spine, or there is evidence of distant metastases via hematogenous or lymphatic spread (**Fig. 11**).[35,36] Such lesions are found during initial work-up of the primary lesion or are observed as progression or recurrence following treatment of the original lesion.[37]

METASTATIC LESIONS TO THE PITUITARY

Metastasis to the pituitary gland is a rare finding in a typical neuroradiologic practice. The incidence of metastatic lesions to the pituitary gland may be as low as 1% in some surgical series.[37] Autopsy series in the setting of widely metastatic disease have suggested higher incidence, ranging from 3% to 27%.[38] The rich vascularity of the pituitary gland presumably facilitates hematogenous transport, implantation, and growth of micrometastases. Breast and lung cancers are the most common primary malignancies associated with pituitary metastases, accounting for 37% and 25%, respectively.[39] Although most metastases to pituitary gland are asymptomatic, they can present with clinical symptoms, most commonly panhypopituitarism or diabetes insipidus.[38] Occasionally, metastasis to the pituitary gland may occur as the initial manifestation of metastatic disease. In one report, pituitary metastasis was the presenting lesion in more than half the patients, with a variety of symptoms, including diabetes insipidus, visual field defects, cranial nerve abnormalities, or headache.[40]

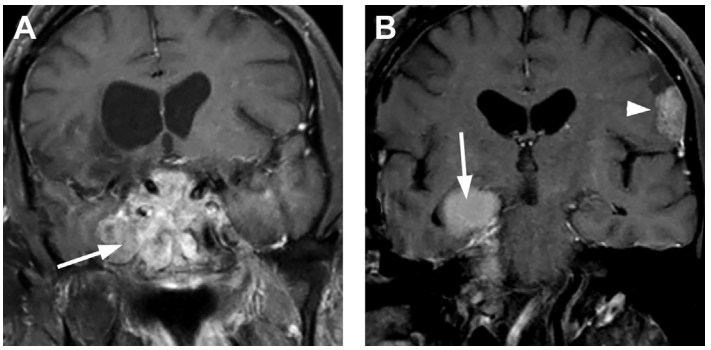

Fig. 11. Pituitary carcinoma. A 69-year-old patient with persistent pituitary adenoma despite surgical and radiation treatments. (*A*) Coronal postcontrast T1-weighted MR image shows persistent tumor invading the skull base and cavernous sinuses (*arrow*). (*B*) Coronal postcontrast T1-weighted image shows invasion of mass into right temporal lobe (*arrow*) and a new left frontal convexity mass (*arrowhead*), consistent with leptomeningeal spread.

The MR imaging and CT features of metastatic disease to the pituitary gland are largely nonspecific. Often, metastatic disease may appear similar to macroadenomas, creating a diagnostic dilemma.[41] Clues that suggest metastasis to pituitary include a new pituitary mass that develops during metastatic surveillance, presence of additional metastatic foci, or if a suspected incidental adenoma in a patients with cancer undergoes rapid growth and becomes symptomatic. CT may demonstrate a sellar mass that is isodense or hyperdense, and associated with heterogeneous enhancement. The clinoid processes or bony sellar floor may be eroded.[39] Also, the tumor can extend into the suprasellar space or laterally into the cavernous sinus. MR imaging can have an appearance indistinguishable from adenoma (**Fig. 12**). The lesion can show heterogeneous signal related to intrinsic necrosis or hemorrhage, variable enhancement, and the margins of the lesion may be slightly more irregular than macroadenoma.[42]

PITUITARY HYPERPLASIA

Pituitary hyperplasia is simply defined as the nonneoplastic increase in the number of pituitary cells. If this hyperplasia is significant, the gland can demonstrate an increase in overall size. This can be a normal physiologic response and does not necessarily indicate pathology. For example, the pituitary gland normally increases in size during pregnancy because of hyperplasia of prolactin cells. Hyperplasia can also occur in pathologic conditions. With primary hypothyroidism, there is a lack of circulating thyroxine. With decreased thyroxine, the hypothalamus produces excess thyrotropin-releasing hormone, which stimulates the thyrotrophs of the anterior pituitary and produces pituitary enlargement. The associated diffuse enlargement of the anterior lobe of pituitary gland can mimic the appearance of pituitary macroadenoma, with an enhancing sellar and suprasellar mass.[43] With adequate hormone replacement, follow-up studies show normalization of the pituitary gland (**Fig. 13**).

RATHKE CLEFT CYST

Rathke cleft cyst is a nonneoplastic lesion arising from remnants of the embryologic Rathke pouch and generally presents as an asymptomatic cyst in the sella with or without suprasellar extension. Famini and colleagues[35] examined brain MR imaging findings in 2598 patients and found an incidence of 3.4%. Rarely, such cysts are symptomatic with the most common complaint being headache, followed by visual disturbance and pituitary dysfunction. The cyst wall is a delicate epithelial wall made of simple or

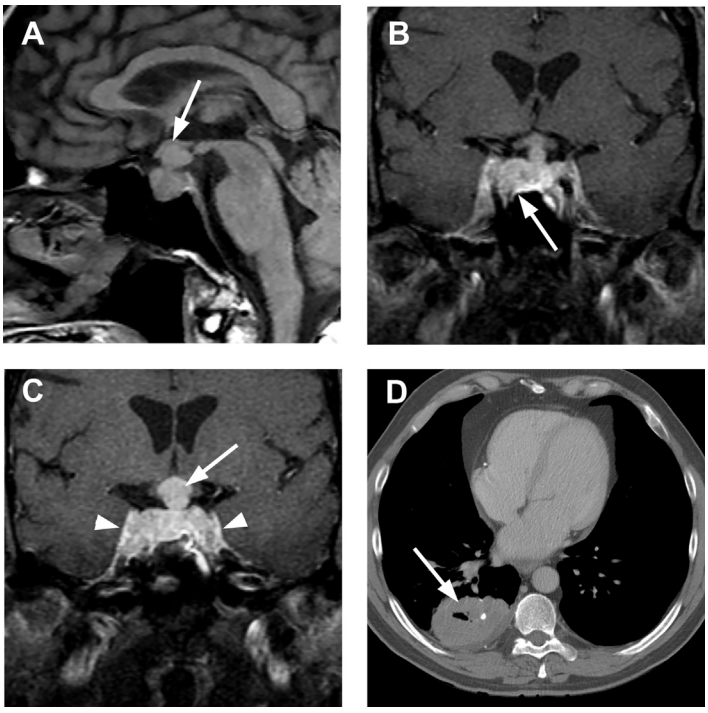

Fig. 12. Metastatic non–small cell lung cancer. A 60-year-old man with no prior history presented with severe headache for 1 month, found to have diabetes insipidus and panhypopituitarism. (*A*) Sagittal T1-weighted MR imaging shows sellar and suprasellar mass effacing optic chiasm (*arrow*). (*B*) Coronal postcontrast T1-weighted image shows asymmetric enlargement of the pituitary gland (*arrow*). (*C*) Coronal postcontrast T1-weighted image slightly more posterior shows marked enlargement of infundibulum (*arrow*) and bilateral cavernous sinus infiltration (*arrowheads*). (*D*) Contrast-enhanced chest CT demonstrated primary lung cancer right lower lobe (*arrow*).

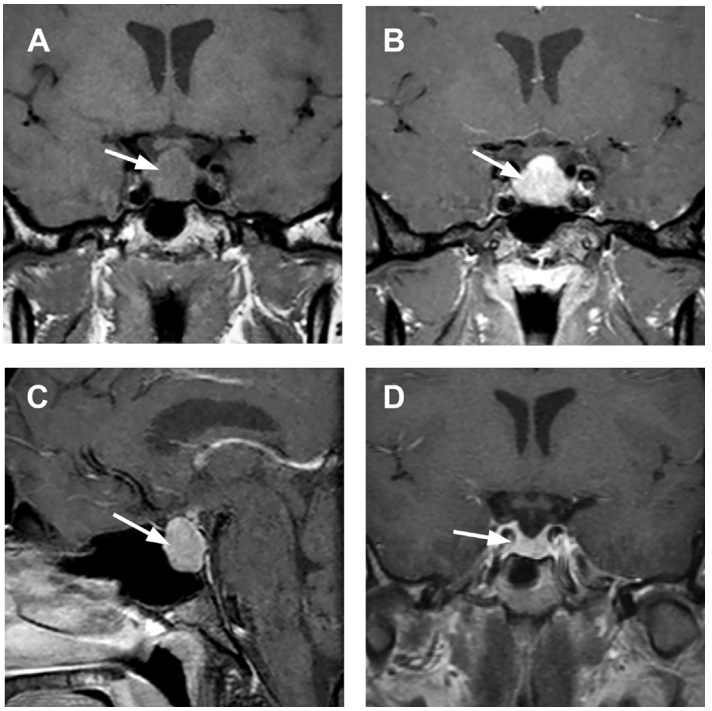

Fig. 13. Pituitary hyperplasia secondary to hypothyroidism. A 32-year-old woman with history of obesity and hypothyroidism was treated with thyroid-replacement therapy, and presented with vague symptoms of headache, nausea, and blurred vision. She had stopped her thyroid-replacement therapy 4 months earlier. (*A*) Coronal unenhanced T1-weighted MR image demonstrates mass-like enlargement of pituitary gland (*arrow*) contacting optic chiasm. (*B*, *C*) Coronal and sagittal postcontrast T1-weighted images show homogeneous enhancement of enlarged pituitary gland (*arrow*), similar to appearance of a macroadenoma. (*D*) Follow-up study after resumption of thyroid hormone replacement shows marked decrease in size of pituitary gland (*arrow*).

pseudostratified cuboidal or columnar cells and may contain cilia and goblet cells. The cyst generally contains mucoid or gelatinous material and can have fluid of variable consistency. CT demonstrates homogenous masses of variable density relative to brain, with 10% to 15% containing peripheral calcification. MR imaging demonstrates a nonenhancing cystic lesion that is variable in signal depending on contents of the cyst. On T1-weighted images, approximately 50% are hyperintense and the other 50% hypointense (**Fig. 14**). On T2-weighted images, 70% are hyperintense and 30% isointense/hypointense. Some lesions contain a small intracystic nodule that is typically hyperintense on T1, hypointense on T2, and shows enhancement.[44]

CRANIOPHARYNGIOMA

Craniopharyngiomas are rare epithelial tumors that arise from the Rathke pouch and occur along the path of the craniopharyngeal duct. These lesions typically occur in a suprasellar location (75%–90%) and involve the infundibulum. However, 20% of craniopharyngiomas show suprasellar and sellar components and 5% are intrasellar in location.[45] Although the lesions are histologically benign, they can be locally aggressive and cause significant morbidity. Symptoms in childhood cases are dominated by nonspecific manifestations of intracranial pressure (headache, nausea, and vomiting). Visual impairment (62%–84%) and endocrine deficits, such as GH deficiency (52%–87%), are also common. In adult cases, patients also present with visual field deficits and headache. The hormonal deficits in adults are more pronounced when compared with childhood-onset cases. At the time of diagnosis, 40% to 87% of patients present with at least one hormonal deficit. Endocrine deficits are found with GH secretion (75%), gonadotropins (40%), ACTH (25%), and TSH (25%). Diabetes insipidus is found in 17% to 27%.[46]

There are two broad types of craniopharyngiomas. Adamantinomatous lesions are more common in childhood, generally present as heterogeneous solid and cystic lesions, and are associated with calcifications identified on CT in 90% of cases. The solid components generally enhance, whereas the cystic components do not enhance and show heterogeneous, often complex signal (**Fig. 15**). The papillary type is more typically solid, enhance, rarely show calcification, and are the most common type found in adulthood (**Fig. 16**). When evaluating craniopharyngiomas on MR imaging, it is important to identify the full extent of the tumor preoperatively, establishing the relationship of the tumor to the surrounding structures including the optic chiasm, the chiasmatic cistern, the third ventricle, the stalk, and the hypothalamus.[47]

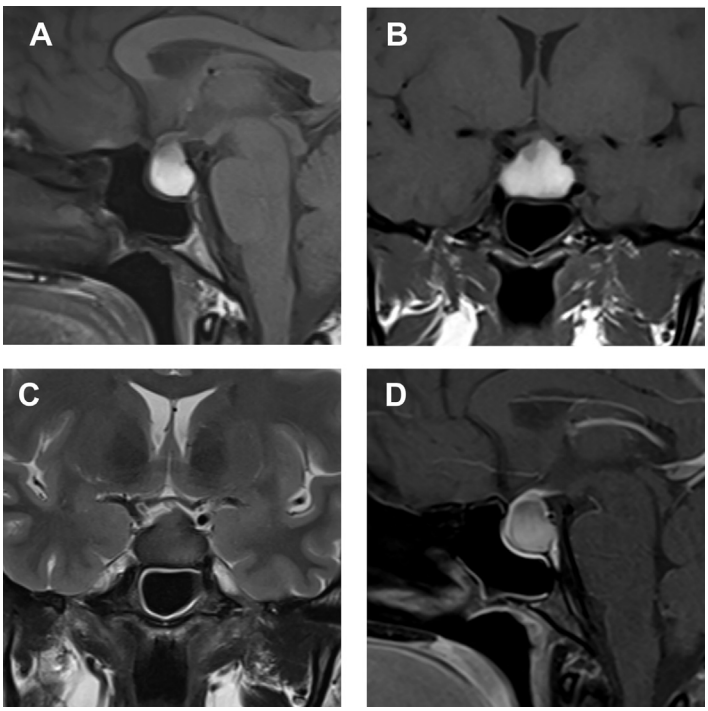

Fig. 14. Rathke cleft cyst. A 39-year-old woman with incidentally discovered sellar mass. (*A*, *B*) Sagittal and coronal T1-weighted unenhanced MR imaging demonstrates large cystic sellar and suprasellar lesion that is T1 hyperintense, secondary to proteinaceous contents. (*C*) Coronal T2-weighted image demonstrates diffuse hypointensity of the lesion. (*D*) Sagittal postcontrast T1-weighted image shows no nodular enhancing tissue.

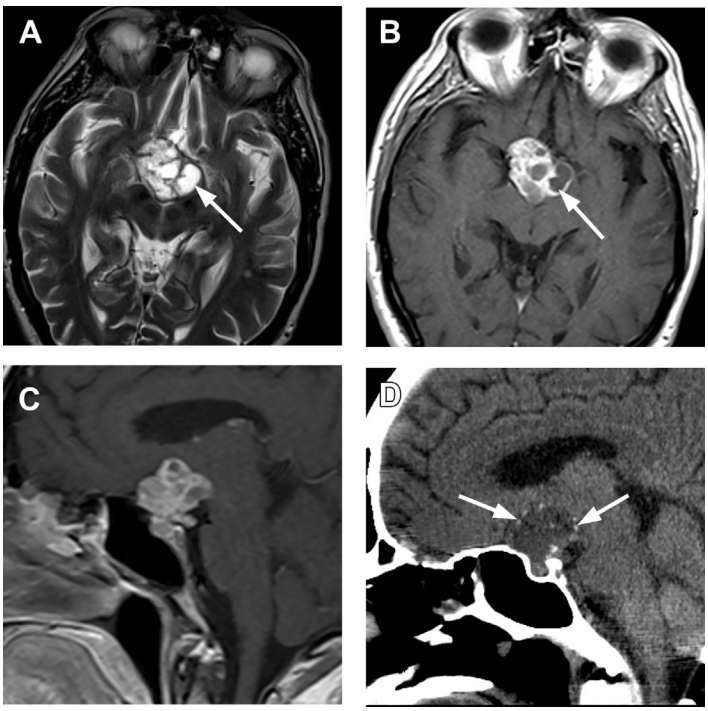

Fig. 15. Craniopharyngioma, adamantinomatous type. A 68-year-old man presented with bitemporal vison loss. (*A*) Axial T2-weighted MR imaging shows suprasellar lesion with multiple cystic areas (*arrow*). (*B*) Axial enhanced T1-weighted MR imaging demonstrates complex sellar and suprasellar lesion with enhancing solid and cystic components (*arrow*). (*C*) Sagittal enhanced T1-weighted MR imaging demonstrates multilobular appearance. (*D*) Sagittal CT identifies punctate calcifications around the margin of the lesion (*arrows*), characteristic of craniopharyngioma.

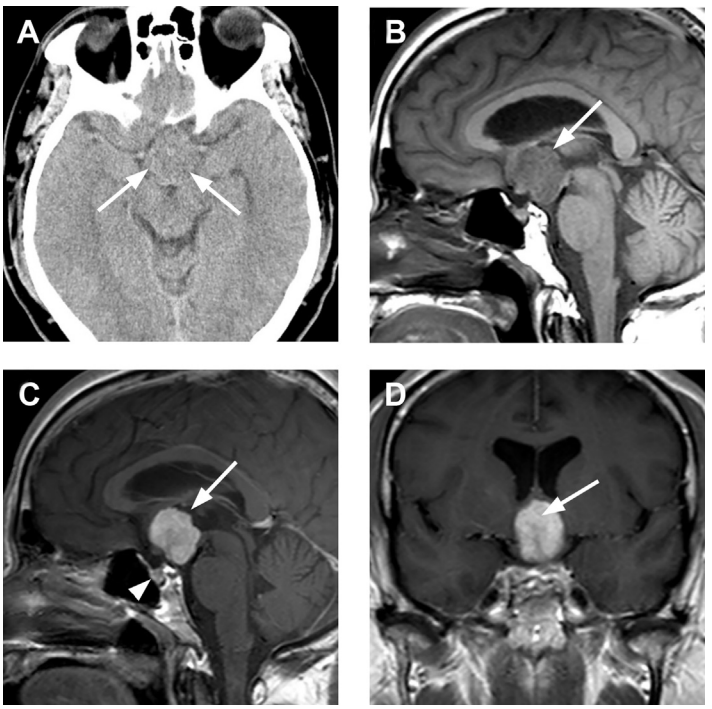

Fig. 16. Craniopharyngioma, papillary type. A 57-year-old man presented acutely with transient episode of tunnel vison and diplopia. (*A*) Axial CT demonstrates 3.0-cm isodense suprasellar mass (*arrows*) without calcifications. (*B*) Sagittal T1-weighted MR demonstrates large suprasellar mass that obscures the pituitary stalk, pushes the chiasm anteriorly, and extends into the anterior third ventricle (*arrow*). (*C*, *D*) Sagittal and coronal postcontrast T1-weighted MR images show homogeneously enhancing suprasellar mass (*arrows*). Note the normal appearing enhancing pituitary tissue in sella (*arrowhead* in *C*).

GERMINOMA/GERM CELL TUMORS

Germinoma is the most common (67%) of intracranial germ cell tumors. Most tumors occur in children and adolescents, and most occur before age 20.[48] Although germinomas are most commonly located in the pineal region and affect males, 20% to 40% arise in the suprasellar region and more commonly occur in females.[49] Tumors that involve both regions at presentation are termed "bifocal," and the incidence of bifocal germinoma ranges from 2% to 41%.[50] Suprasellar lesions are locally invasive and can invade the infundibulum, the chiasm, and hypothalamus. Distinction from other nongerminomatous germ cell tumors is determined histologically and through evaluation of protein markers in cerebrospinal fluid. Suprasellar germinomas often present with diabetes insipidus and other endocrine deficiencies. Visual disturbance and obstructive hydrocephalus can occur. Germinomas can spread easily through cerebrospinal fluid dissemination, and imaging of the entire neuroaxis is warranted for staging. On CT, lesions are isodense to hyperdense to brain parenchyma and rarely demonstrate calcification or osseous invasion. MR imaging typically shows an ill-defined enhancing mass in the region of the infundibulum that invades and compresses the chiasm and third ventricle (**Fig. 17**).[49]

PITUICYTOMA

Pituicytoma is a rare World Health Organization grade I sellar and/or suprasellar neoplasm presumably derived from neurohypophyseal pituicytes.[51] These lesions are similar to adenomas on conventional MR imaging, demonstrating T1 isointensity, heterogeneous hyperintensity on T2-weighted images, and heterogeneous enhancement. No distinctive imaging features can confidently allow preoperative diagnosis. These lesions represent a unique surgical subgroup, and resection is associated with significant morbidity including increased intraoperative hemorrhage, diabetes insipidus, and panhypopituitarism (**Fig. 18**).[52]

MENINGIOMA

Meningiomas arise from arachnoid cap cells and can occur anywhere that meninges are found; 10% to 15% involve the sella and parasellar regions.[53] Most meningiomas are benign, World Health Organization grade I lesions based on histologic subtype and lack of anaplastic features. Grade II meningiomas are atypical, and grade III meningiomas are considered anaplastic or malignant. Midline meningiomas of the skull base are challenging in terms of diagnosis and management given their proximity to the pituitary gland,

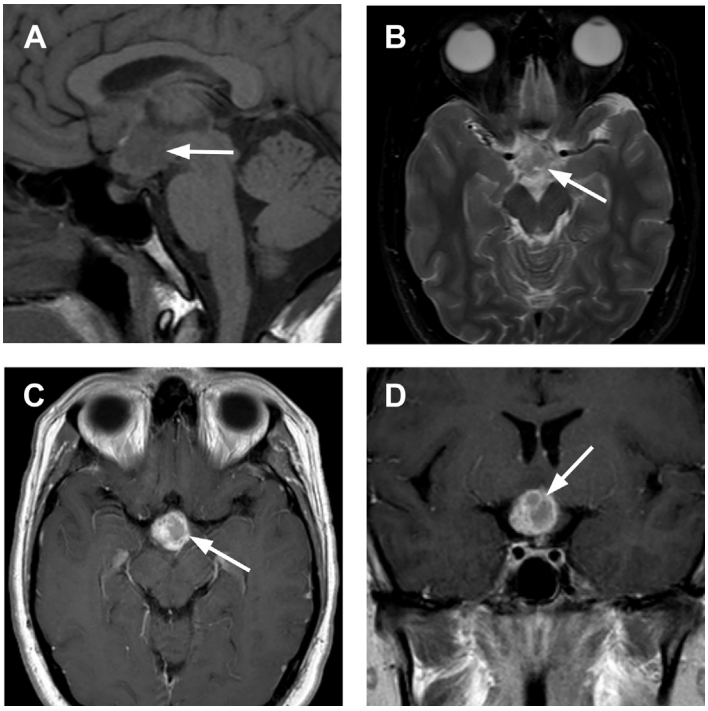

Fig. 17. Suprasellar germ cell tumor. A 20 year old with panhypopituitarism presents with recent worsening in peripheral vision. (*A*) Sagittal T1-weighted MR imaging shows large isointense suprasellar mass (*arrow*). (*B*) Axial T2-weighted image shows lobular T2 hyperintense suprasellar lesion (*arrow*). (*C, D*) Axial and coronal enhanced T1-weighted images show the rounded mass is heterogeneously enhancing (*arrows*). Elevated cerebrospinal a-fetoprotein and human chorionic gonadotropin (HCG) were noted, indicating that the lesion is not pure germinoma.

cavernous sinus, carotid vessels, and cranial nerves. Meningiomas can have a variety of growth patterns ranging from pedunculated focal mass to en plaque dural infiltration.

High-resolution CT or MR imaging is often necessary to separate an enhancing tumor from adjacent enhancing structures including the cavernous sinus or pituitary gland. Fat-saturation sequences are also invaluable in distinguishing an enhancing tumor from skull base fat on T1-weighted images. The dural tail sign is a common finding but is not pathognomonic. Meningiomas can encase the ICA and result in narrowing. In contrast, pituitary adenomas that surround the ICA usually do not significantly constrict or occlude the vessel.

The effect of meningioma growth on underlying skull base is variable. Most meningiomas do not cause obvious changes in the underlying bone, but some meningiomas cause hyperostosis. Pieper and colleagues[54] suggested that hyperostosis associated with meningiomas of the skull base demonstrates histologic tumor invasion. Osseous invasion can have a range of appearances, ranging from sclerosis to permeative to lytic.

Meningiomas are variably classified in the literature according to the anatomic site of origin or involvement. Lesions involving the skull base

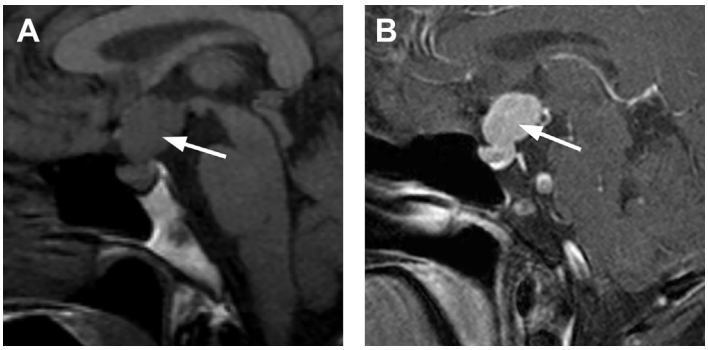

Fig. 18. Pituicytoma. A 60-year-old man presented with trauma. CT showed an incidental sellar and suprasellar mass. (*A*) Sagittal MR imaging shows T1-isointense predominantly suprasellar mass (*arrow*) that displaces optic chiasm and compresses the anterior third ventricle. (*B*) Sagittal postcontrast T1-weighted image demonstrates homogeneous enhancement of the mass (*arrow*).

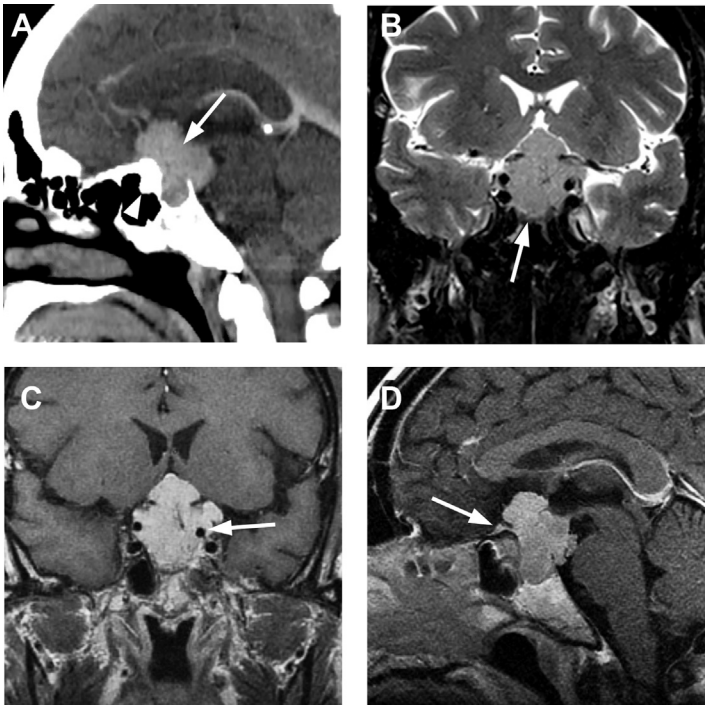

Fig. 19. Meningioma. (*A*) Sagittal reformation of enhanced CT scan shows large sellar and suprasellar enhancing mass (*arrow*). There is expansion of the sella and focal hyperostosis of the tuberculum sella (*arrowhead*). (*B*) Coronal T2-weighted MR imaging shows multilobulated mass. Compressed pituitary tissue is identified along floor of sella (*arrow*). (*C*) Coronal postcontrast T1-weighted image shows avid enhancement of the meningioma. There are multiple encased vessels including left supraclinoid carotid artery (*arrow*). (*D*) Sagittal postcontrast T1-weighted image shows large lobulated lesion with subtle dural tail (*arrow*) along planum sphenoidale.

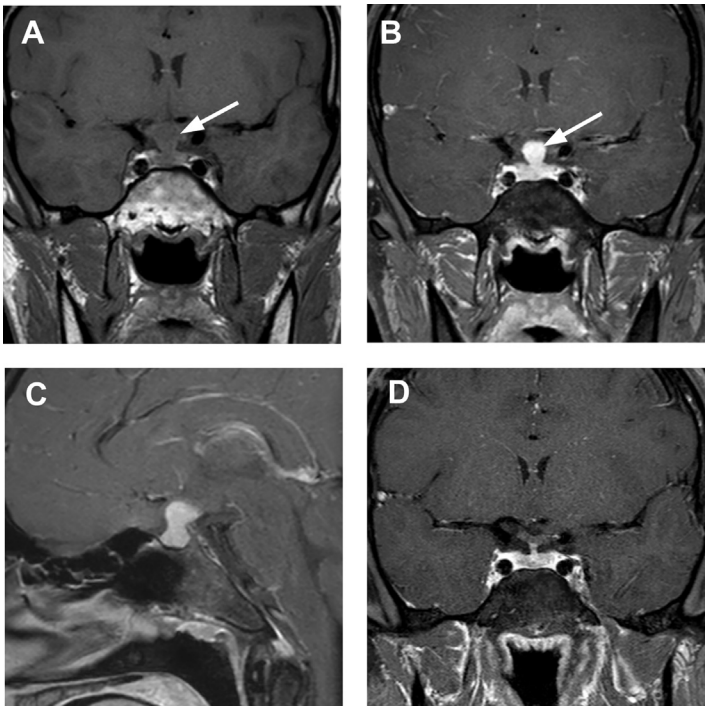

Fig. 20. Primary hypophysitis. A 20 year old presented with headache, blurred vision, and 6 months of multiple symptoms related to panhypopituitarism. (*A*) Coronal T1-weighted unenhanced MR image shows marked enlargement of infundibulum (*arrow*). (*B*) Coronal enhanced T1-weighted image shows marked enhancement of the enlarged infundibulum (*arrow*). (*C*) Sagittal enhanced T1-weighted image shows the process involves the pituitary and the infundibulum. (*D*) After temporary treatment with steroids, the 1-year follow-up coronal enhanced T1-weighted image shows normalization of the infundibulum.

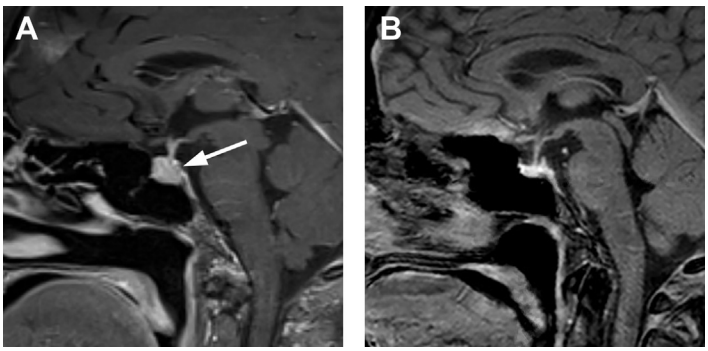

Fig. 21. Ipilumimab-related hypophysitis. A 55 year old with metastatic melanoma was treated with four doses of combination ipilumimab and nivolumab and developed progressive fatigue and adrenal insufficiency. (*A*) Sagittal enhanced T1-weighted MR imaging shows global enlargement of the pituitary gland (*arrow*) and mild enlargement of the stalk. (*B*) Three weeks after steroid therapy, repeat MR imaging showed normalization of the gland.

may be localized to the planum sphenoidale, the sella, cavernous sinus, or clinoid processes. Planum meningiomas can directly arise from the superior surface of the planum. Planum meningiomas, like tuberculum sella meningiomas, can extend laterally to involve the optic nerve canal or superiorly to involve the suprasellar region, resulting in unilateral or bilateral vision loss. Meningiomas primarily involving or largely involving the sella can present with mild elevation of prolactin levels, but most do not have significant endocrine dysfunction preoperatively.[55] Sellar meningiomas is difficult to differentiate from a large macroadenoma. An enhancing dural tail, lesion calcification, or adjacent skull base hyperostosis may suggest meningioma (**Fig. 19**).

HYPOPHYSITIS

Hypophysitis is a broad nonspecific term that includes a diverse group of conditions that result in localized inflammation of the pituitary gland and/or stalk. The associated pituitary gland inflammation can lead to abnormal enlargement of the infundibulum and the gland itself. Hypophysitis has been classified according to etiology, anatomic location, and histologic variants, and elucidation of this classification is beyond the scope of this article.[56] In general, MR imaging of these lesions demonstrates enlargement and intense homogeneous enhancement of the infundibulum and/or gland on dedicated postgadolinium MR imaging sequences, without deviation of the stalk. These lesions are difficult to differentiate radiologically from adenomas or germinomas. Clinically, patients can present with headache, anterior and posterior pituitary deficiencies, and visual defects.

Primary hypophysitis is considered idiopathic, possibly autoimmune in cause; secondary forms are caused by known associated etiologies (medication or systemic disease). The most common primary form is lymphocytic hypophysitis. It is probably autoimmune in nature and typically occurs in females during last month of pregnancy or in early postpartum period. Other forms of primary hypophysitis show similar imaging features and symptoms but are not associated with pregnancy (**Fig. 20**).

One unique form of secondary hypophysitis occurs after therapy with immune checkpoint inhibitors, such as ipilumimab, an established therapy for metastatic melanoma. Patients generally present after three or four infusions, with an incidence that may be 17%.[57] Symptoms are not specific but may include lethargy, headaches, myalgia, or nausea and vomiting. Patients may also have eye pain, diplopia, or other visual defects. Gadolinium-enhanced MR imaging shows diffuse enlargement of the pituitary gland and/or stalk (**Fig. 21**). Treatment with corticosteroids usually results in normalization of the pituitary findings.

SUMMARY

The most common primary lesion of the pituitary gland, sella, and suprasellar region is the adenoma. However, the spectrum of nonadenomatous abnormalities is broad, and a reasonable differential should be considered for each lesion. The pituitary gland is best evaluated with dedicated MR imaging, with CT performing a complementary role in evaluation. For any lesion, it is important to consider location, point of origin, relationship to adjacent structures, and clinical scenario to propose the most appropriate diagnosis.

DISCLOSURE

The authors have nothing to disclose.

REFERENCES

1. Elster AD. Imaging of the sella: anatomy and pathology. Semin Ultrasound CT MR 1993;14(3):182–94.

2. Stobo DB, Lindsay RS, Connell JM, et al. Initial experience of 3 Tesla versus conventional field strength magnetic resonance imaging of small functioning pituitary tumours. Clin Endocrinol (Oxf) 2011;75(5):673–7.
3. Erickson D, Erickson B, Watson R, et al. 3 Tesla magnetic resonance imaging with and without corticotropin releasing hormone stimulation for the detection of microadenomas in Cushing's syndrome. Clin Endocrinol (Oxf) 2010;72(6):793–9.
4. Bladowska J, Sasiadek M. Diagnostic imaging of the pituitary and parasellar region. In: Rahimi-Movaghar PV, editor. Pituitary adenomas. InTech; 2012.
5. Chowdhury IN, Sinaii N, Oldfield EH, et al. A change in pituitary magnetic resonance imaging protocol detects ACTH-secreting tumours in patients with previously negative results. Clin Endocrinol (Oxf) 2010;72(4):502–6.
6. Friedman TC, Zuckerbraun E, Lee ML, et al. Dynamic pituitary MRI has high sensitivity and specificity for the diagnosis of mild Cushing's syndrome and should be part of the initial workup. Horm Metab Res 2007;39(6):451–6.
7. Grober Y, Grober H, Wintermark M, et al. Comparison of MRI techniques for detecting microadenomas in Cushing's disease. J Neurosurg 2018;128(4):1051–7.
8. Kunii N, Abe T, Kawamo M, et al. Rathke's cleft cysts: differentiation from other cystic lesions in the pituitary fossa by use of single-shot fast spin-echo diffusion-weighted MR imaging. Acta Neurochir (Wien) 2007;149(8):759–69 [discussion: 769].
9. Rogg JM, Tung GA, Anderson G, et al. Pituitary apoplexy: early detection with diffusion-weighted MR imaging. AJNR Am J Neuroradiol 2002;23(7):1240–5.
10. Yiping L, Ji X, Daoying G, et al. Prediction of the consistency of pituitary adenoma: a comparative study on diffusion-weighted imaging and pathological results. J Neuroradiol 2016;43(3):186–94.
11. Bou-Ayache JM, Delman BN. Advances in imaging of the pediatric pituitary gland. Endocrinol Metab Clin North Am 2016;45(2):443–52.
12. Chaudhary V, Bano S. Imaging of the pituitary: recent advances. Indian J Endocrinol Metab 2011;15(Suppl 3):S216–23.
13. Di Iorgi N, Allegri AE, Napoli F, et al. The use of neuroimaging for assessing disorders of pituitary development. Clin Endocrinol (Oxf) 2012;76(2):161–76.
14. Zamora C, Castillo M. Sellar and parasellar imaging. Neurosurgery 2017;80(1):17–38.
15. Go JL, Rajamohan AG. Imaging of the sella and parasellar region. Radiol Clin North Am 2017;55(1):83–101.
16. Rennert J, Doerfler A. Imaging of sellar and parasellar lesions. Clin Neurol Neurosurg 2007;109(2):111–24.
17. Shaffi OM, Wrightson P. Dural invasion by pituitary tumours. N Z Med J 1975;81(538):386–90.
18. Trevino R. Chiasmal syndrome. J Am Optom Assoc 1995;66(9):559–75.
19. Lee IH, Miller NR, Zan E, et al. Visual defects in patients with pituitary adenomas: the myth of bitemporal hemianopsia. AJR Am J Roentgenol 2015;205(5):W512–8.
20. Symon L, Jakubowski J, Kendall B. Surgical treatment of giant pituitary adenomas. J Neurol Neurosurg Psychiatry 1979;42(11):973–82.
21. Mohr G, Hardy J, Comtois R, et al. Surgical management of giant pituitary adenomas. Can J Neurol Sci 1990;17(1):62–6.
22. Songtao Q, Yuntao L, Jun P, et al. Membranous layers of the pituitary gland: histological anatomic study and related clinical issues. Neurosurgery 2009;64(3 Suppl):ons1–9 [discussion: ons9–10].
23. Knosp E, Steiner E, Kitz K, et al. Pituitary adenomas with invasion of the cavernous sinus space: a magnetic resonance imaging classification compared with surgical findings. Neurosurgery 1993;33(4):610–7 [discussion: 617–18].
24. Cottier JP, Destrieux C, Brunereau L, et al. Cavernous sinus invasion by pituitary adenoma: MR imaging. Radiology 2000;215(2):463–9.
25. Selman WR, Laws ER Jr, Scheithauer BW, et al. The occurrence of dural invasion in pituitary adenomas. J Neurosurg 1986;64(3):402–7.
26. Meij BP, Lopes MB, Ellegala DB, et al. The long-term significance of microscopic dural invasion in 354 patients with pituitary adenomas treated with transsphenoidal surgery. J Neurosurg 2002;96(2):195–208.
27. Luo CB, Teng MM, Chen SS, et al. Imaging of invasiveness of pituitary adenomas. Kaohsiung J Med Sci 2000;16(1):26–31.
28. Chen X, Dai J, Ai L, et al. Clival invasion on multidetector CT in 390 pituitary macroadenomas: correlation with sex, subtype and rates of operative complication and recurrence. AJNR Am J Neuroradiol 2011;32(4):785–9.
29. Barkhoudarian G, Kelly DF. Pituitary apoplexy. Neurosurg Clin N Am 2019;30(4):457–63.
30. Wildemberg LE, Glezer A, Bronstein MD, et al. Apoplexy in nonfunctioning pituitary adenomas. Pituitary 2018;21(2):138–44.
31. Semple PL, Jane JA, Lopes MB, et al. Pituitary apoplexy: correlation between magnetic resonance imaging and histopathological results. J Neurosurg 2008;108(5):909–15.
32. Burns J, Policeni B, Bykowski J, et al. ACR Appropriateness Criteria Neuroendocrine Imaging. Expert panel on neurologic imaging. J Am Coll Radiol 2019;16(5S):S161–73.
33. Dubuisson AS, Beckers A, Stevenaert A. Classical pituitary tumour apoplexy: clinical features,

management and outcomes in a series of 24 patients. Clin Neurol Neurosurg 2007;109(1):63–70.
34. Kasuki L, Raverot G. Definition and diagnosis of aggressive pituitary tumors. Rev Endocr Metab Disord 2020;21(2):203–8.
35. Famini P, Maya MM, Melmed S. Pituitary magnetic resonance imaging for sellar and parasellar masses: ten-year experience in 2598 patients. J Clin Endocrinol Metab 2011;96(6):1633–41.
36. Ragel BT, Couldwell WT. Pituitary carcinoma: a review of the literature. Neurosurg Focus 2004; 16(4):E7.
37. Sansur CA, Oldfield EH. Pituitary carcinoma. Semin Oncol 2010;37(6):591–3.
38. Di Nunno V, Mollica V, Corcioni B, et al. Clinical management of a pituitary gland metastasis from clear cell renal cell carcinoma. Anticancer Drugs 2018; 29(7):710–5.
39. Angelousi A, Alexandraki KI, Kyriakopoulos G, et al. Neoplastic metastases to the endocrine glands. Endocr Relat Cancer 2020;27(1):R1–20.
40. Morita A, Meyer FB, Laws ER Jr. Symptomatic pituitary metastases. J Neurosurg 1998;89(1):69–73.
41. Spinelli GP, Lo Russo G, Miele E, et al. Breast cancer metastatic to the pituitary gland: a case report. World J Surg Oncol 2012;10:137.
42. He W, Chen F, Dalm B, et al. Metastatic involvement of the pituitary gland: a systematic review with pooled individual patient data analysis. Pituitary 2015;18(1):159–68.
43. Al-Gahtany M, Horvath E, Kovacs K. Pituitary hyperplasia. Hormones (Athens) 2003;2(3):149–58.
44. Larkin S, Karavitaki N, Ansorge O. Rathke's cleft cyst. Handb Clin Neurol 2014;124:255–69.
45. Zada G, Lin N, Ojerholm E, et al. Craniopharyngioma and other cystic epithelial lesions of the sellar region: a review of clinical, imaging, and histopathological relationships. Neurosurg Focus 2010;28(4):E4.
46. Muller HL. Craniopharyngioma. Endocr Rev 2014; 35(3):513–43.
47. Prieto R, Pascual JM, Barrios L. Topographic diagnosis of craniopharyngiomas: the accuracy of MRI findings observed on conventional T1 and T2 images. AJNR Am J Neuroradiol 2017;38(11):2073–80.
48. Osorio DS, Allen JC. Management of CNS germinoma. CNS Oncol 2015;4(4):273–9.
49. Chung EM, Biko DM, Schroeder JW, et al. From the radiologic pathology archives: precocious puberty: radiologic-pathologic correlation. Radiographics 2012;32(7):2071–99.
50. Lee L, Saran F, Hargrave D, et al. Germinoma with synchronous lesions in the pineal and suprasellar regions. Childs Nerv Syst 2006;22(12):1513–8.
51. Viaene AN, Lee EB, Rosenbaum JN, et al. Histologic, immunohistochemical, and molecular features of pituicytomas and atypical pituicytomas. Acta Neuropathol Commun 2019;7(1):69.
52. Guerrero-Perez F, Marengo AP, Vidal N, et al. Primary tumors of the posterior pituitary: a systematic review. Rev Endocr Metab Disord 2019;20(2): 219–38.
53. FitzPatrick M, Tartaglino LM, Hollander MD, et al. Imaging of sellar and parasellar pathology. Radiol Clin North Am 1999;37(1):101–21, x.
54. Pieper DR, Al-Mefty O, Hanada Y, et al. Hyperostosis associated with meningioma of the cranial base: secondary changes or tumor invasion. Neurosurgery 1999;44(4):742–6 [discussion: 746–7].
55. Sathananthan M, Sathananthan A, Scheithauer BW, et al. Sellar meningiomas: an endocrinologic perspective. Pituitary 2013;16(2):182–8.
56. Faje A. Hypophysitis: evaluation and management. Clin Diabetes Endocrinol 2016;2:15.
57. Dillard T, Yedinak CG, Alumkal J, et al. Anti-CTLA-4 antibody therapy associated autoimmune hypophysitis: serious immune related adverse events across a spectrum of cancer subtypes. Pituitary 2010;13(1): 29–38.